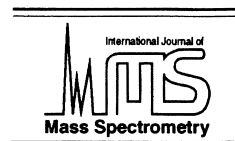




ELSEVIER

International Journal of Mass Spectrometry 204 (2001) 296–299



Subject index

Alcohols

Intrinsic reactivity of metal–hydroxide complexes: O–H bond activation and adduct formation in gas-phase reactions of Cp_2ZrOH^+ , 255

Alkali cation

Reactions of multidentate ligands with ligated alkali cation complexes: self-exchange and “sandwich” complex formation kinetics of gas phase crown ether–alkali cation complexes, 171

Amides

Intrinsic reactivity of metal–hydroxide complexes: O–H bond activation and adduct formation in gas-phase reactions of Cp_2ZrOH^+ , 255

Amino acids

Chiral resolution of D- and L-amino acids by tandem mass spectrometry of Ni(II)-bound trimeric complexes, 159

Associative ionization

Associative ionization of excited sodium species with various ligands: assessing relative bonding strengths of ion–ligand interactions, 247

Binding selectivity

Determination of alkali metal binding selectivities of caged crown ligands by electrospray ionization quadrupole ion trap mass spectrometry, 133

Bond activation

Structure and reactivity of the prototype iron–oxide cluster Fe_2O_2^+ , 233

Bond energies

Determination of weak $\text{Fe}^+\text{–L}$ bond energies ($\text{L} = \text{Ar}, \text{Kr}, \text{Xe}, \text{N}_2,$ and CO_2) by ligand exchange reactions and collision-induced dissociation, 7

Photodissociation measurements of bond dissociation energies: $D_0(\text{Al}_2\text{–Al})$, $D_0(\text{TiO}^+\text{–Mn})$, and $D_0(\text{V}_+^2\text{–V})$, 143

(*c*-C₅H₅)Fe⁺ cation reactivity

Coordination chemistry of (*c*-C₅H₅)Fe⁺ in the gas phase at $294 \pm \text{K}$: reactions with the inorganic ligands H₂, H₂O, NH₃, CO, N₂, NO, CO₂, N₂O, and NO₂, 209

Chirality

Chiral resolution of D- and L-amino acids by tandem mass spectrometry of Ni(II)-bound trimeric complexes, 159

CID technique

Coordination chemistry of (*c*-C₅H₅)Fe⁺ in the gas phase at $294 \pm \text{K}$: reactions with the inorganic ligands H₂, H₂O, NH₃, CO, N₂, NO, CO₂, N₂O, and NO₂, 209

Clusters

Chiral resolution of D- and L-amino acids by tandem mass spectrometry of Ni(II)-bound trimeric complexes, 159

Photodissociation of exohedral transition metal–C₆₀ complexes, 223

Sigma bond activation by transition metal ions: the $\text{Co}(\text{CH}_4)_n^+$ systems revisited, 281

Clusters ions

Associative ionization of excited sodium species with various ligands: assessing relative bonding strengths of ion–ligand interactions, 247

Collision-induced dissociation

Determination of weak $\text{Fe}^+\text{–L}$ bond energies ($\text{L} = \text{Ar}, \text{Kr}, \text{Xe}, \text{N}_2,$ and CO_2) by ligand exchange reactions and collision-induced dissociation, 7

Investigation of metal complex coordination structure using collision-induced dissociation and ion–molecule reactions in a quadrupole ion trap mass spectrometer, 101

Coordination number

Investigation of metal complex coordination structure using collision-induced dissociation and ion–molecule reactions in a quadrupole ion trap mass spectrometer, 101

Crown ether

Determination of alkali metal binding selectivities of caged crown ligands by electrospray ionization quadrupole ion trap mass spectrometry, 133

Reactions of multidentate ligands with ligated alkali cation complexes: self-exchange and “sandwich” complex formation kinetics of gas phase crown ether–alkali cation complexes, 171

Dissociation energy

Photodissociation measurements of bond dissociation energies: $D_0(\text{Al}_2\text{–Al})$, $D_0(\text{TiO}^+\text{–Mn})$, and $D_0(\text{V}_+^2\text{–V})$, 143

σ -donating ligands

Coordination chemistry of (*c*-C₅H₅)Fe⁺ in the gas phase at $294 \pm \text{K}$: reactions with the inorganic ligands H₂, H₂O, NH₃, CO, N₂, NO, CO₂, N₂O, and NO₂, 209

Electrospray

- Investigation of metal complex coordination structure using collision-induced dissociation and ion–molecule reactions in a quadrupole ion trap mass spectrometer, 101
- Large anhydrous polyalanine ions: substitution of Na^+ for H^+ destabilizes folded states, 87
- Electrospray ionization (ESI)
- Determination of alkali metal binding selectivities of caged crown ligands by electrospray ionization quadrupole ion trap mass spectrometry, 133
- Differences between positive and negative ion stabilities of metal–sulfur cluster proteins: an electrospray ionization Fourier transform ion cyclotron resonance study, 77
- Dissociation mechanisms for metal N-glycosides of N-acetyl neuraminic acid, 185
- Probing protein–metal ion interactions by electrospray ionization mass spectrometry: enolase and nucleocapsid protein, 113
- Structures and fragmentations of zinc(II) complexes of amino acids in the gas phase. II. Decompositions of glycine–Zn(II) complexes, 267
- Enantiomeric excess
- Chiral resolution of D- and L-amino acids by tandem mass spectrometry of Ni(II)-bound trimeric complexes, 159
- Enolase
- Probing protein–metal ion interactions by electrospray ionization mass spectrometry: enolase and nucleocapsid protein, 113
- Esters
- Intrinsic reactivity of metal–hydroxide complexes: O–H bond activation and adduct formation in gas-phase reactions of Cp_2ZrOH^+ , 255
- Excited sodium species
- Associative ionization of excited sodium species with various ligands: assessing relative bonding strengths of ion–ligand interactions, 247
- Fourier transform ion cyclotron resonance (FTICR)
- Differences between positive and negative ion stabilities of metal–sulfur cluster proteins: an electrospray ionization Fourier transform ion cyclotron resonance study, 77
- Investigating the effect of transition metal ion oxidation state on oligodeoxyribonucleotide binding by matrix-assisted laser desorption/ionization Fourier transform ion cyclotron resonance mass spectrometry, 55
- Fourier transform ion cyclotron resonance mass spectrometry (FTICR-MS)
- Structure and reactivity of the prototype iron–oxide cluster Fe_2O_2^+ , 233
- Fourier transform mass spectrometry (FTMS)
- A new external ionization multisample MALDI source for Fourier transform mass spectrometry, 23
- Fragmentation
- Gas-phase ion/ion interactions between peptides/proteins and iron ions in a quadrupole ion trap, 47
- Gas phase
- Gas-phase ion/ion interactions between peptides/proteins and iron ions in a quadrupole ion trap, 47
- Glycine–Zn(II) complexes
- Structures and fragmentations of zinc(II) complexes of amino acids in the gas phase. II. Decompositions of glycine–Zn(II) complexes, 267
- Host–guest chemistry
- Determination of alkali metal binding selectivities of caged crown ligands by electrospray ionization quadrupole ion trap mass spectrometry, 133
- Hydrolysis
- Intrinsic reactivity of metal–hydroxide complexes: O–H bond activation and adduct formation in gas-phase reactions of Cp_2ZrOH^+ , 255
- Hypervalent species
- Complexes of Li atoms with water and ammonia: a combined neutralization–reionization mass spectrometry and theoretical study, 125
- Ion–ion reactions
- Gas-phase ion/ion interactions between peptides/proteins and iron ions in a quadrupole ion trap, 47
- Ion–molecule reactions
- Coordination chemistry of $(c\text{-H}_5\text{H}_5)\text{Fe}^+$ in the gas phase at $294 \pm \text{K}$: reactions with the inorganic ligands H_2 , H_2O , NH_3 , CO , N_2 , NO , CO_2 , N_2O , and NO_2 , 209
- Investigation of metal complex coordination structure using collision-induced dissociation and ion–molecule reactions in a quadrupole ion trap mass spectrometer, 101
- Ion mobility
- Large anhydrous polyalanine ions: substitution of Na^+ for H^+ destabilizes folded states, 87
- Iron
- Determination of weak $\text{Fe}^+\text{-L}$ bond energies ($\text{L} = \text{Ar}$, Kr , Xe , N_2 , and CO_2) by ligand exchange reactions and collision-induced dissociation, 7
- Iron oxide
- Structure and reactivity of the prototype iron–oxide cluster Fe_2O_2^+ , 233
- Kinetics
- Chiral resolution of D- and L-amino acids by tandem mass spectrometry of Ni(II)-bound trimeric complexes, 159
- Reactions of multidentate ligands with ligated alkali cation complexes: self-exchange and “sandwich” complex formation kinetics of gas phase crown ether–alkali cation complexes, 171

Li-atom complexes

Complexes of Li atoms with water and ammonia: a combined neutralization–reionization mass spectrometry and theoretical study, 125

Ligand exchange

Reactions of multidentate ligands with ligated alkali cation complexes: self-exchange and “sandwich” complex formation kinetics of gas phase crown ether–alkali cation complexes, 171

Ligand exchange reactions

Determination of weak $\text{Fe}^+\text{-L}$ bond energies ($\text{L} = \text{Ar}, \text{Kr}, \text{Xe}, \text{N}_2, \text{and CO}_2$) by ligand exchange reactions and collision-induced dissociation, 7

Mass spectrometry

Dissociation mechanisms for metal N-glycosides of N-acetyl neuraminic acid, 185

Gas-phase ion/ion interactions between peptides/proteins and iron ions in a quadrupole ion trap, 47

Investigating the effect of transition metal ion oxidation state on oligodeoxyribonucleotide binding by matrix-assisted laser desorption/ionization Fourier transform ion cyclotron resonance mass spectrometry, 55

Matrix-assisted laser desorption/ionization (MALDI)

Investigating the effect of transition metal ion oxidation state on oligodeoxyribonucleotide binding by matrix-assisted laser desorption/ionization Fourier transform ion cyclotron resonance mass spectrometry, 55

A new external ionization multisample MALDI source for Fourier transform mass spectrometry, 23

Metal binding

Probing protein–metal ion interactions by electrospray ionization mass spectrometry: enolase and nucleocapsid protein, 113

Metal–hydroxide

Intrinsic reactivity of metal–hydroxide complexes: O–H bond activation and adduct formation in gas-phase reactions of Cp_2ZrOH^+ , 255

Metal–ligand interactions

Photodesorption of carbonyl from $\text{Pt}_3(\text{CO})_n^-$ ($n = 1 - 6$), 197

Metal–oxide clusters

Structure and reactivity of the prototype iron–oxide cluster Fe_2O_2^+ , 233

Metal ion binding

Investigating the effect of transition metal ion oxidation state on oligodeoxyribonucleotide binding by matrix-assisted laser desorption/ionization Fourier transform ion cyclotron resonance mass spectrometry, 55

Metal ion–ligand complex

Investigation of metal complex coordination structure using collision-induced dissociation and ion–molecule reactions in a quadrupole ion trap mass spectrometer, 101

Metal ion flux

Stoichiometry in zinc ion transfer from metallothionein to zinc finger peptides, 1

Metallo–fullerenes

Photodissociation of exohedral transition metal– C_{60} complexes, 223

Metalloproteins

Differences between positive and negative ion stabilities of metal–sulfur cluster proteins: an electrospray ionization Fourier transform ion cyclotron resonance study, 77

Metallothionein

Stoichiometry in zinc ion transfer from metallothionein to zinc finger peptides, 1

Monosaccharide

Dissociation mechanisms for metal N-glycosides of N-acetyl neuraminic acid, 185

MP2 perturbation theory

Determination of copper binding sites in peptides containing basic residues: a combined experimental and theoretical study, 31

Neutralization–reionization

Complexes of Li atoms with water and ammonia: a combined neutralization–reionization mass spectrometry and theoretical study, 125

Nickel complexes

Chiral resolution of D- and L-amino acids by tandem mass spectrometry of Ni(II)-bound trimeric complexes, 159

Noncovalent complexes

Stoichiometry in zinc ion transfer from metallothionein to zinc finger peptides, 1

Nucleocapsid protein

Probing protein–metal ion interactions by electrospray ionization mass spectrometry: enolase and nucleocapsid protein, 113

Oligonucleotides

Investigating the effect of transition metal ion oxidation state on oligodeoxyribonucleotide binding by matrix-assisted laser desorption/ionization Fourier transform ion cyclotron resonance mass spectrometry, 55

Oligosaccharide

A new external ionization multisample MALDI source for Fourier transform mass spectrometry, 23

Photodesorption

Photodesorption of carbonyl from $\text{Pt}_3(\text{CO})_n^-$ ($n = 1 - 6$), 197

Photodissociation

Photodesorption of carbonyl from $\text{Pt}_3(\text{CO})_n^-$ ($n = 1 - 6$), 197

- Photodissociation of exohedral transition metal–C₆₀ complexes, 223
- Platinum cluster carbonyls
- Photodesorption of carbonyl from Pt₃(CO)_n[−] (*n* = 1 – 6), 197
- Polyalanine
- Large anhydrous polyalanine ions: substitution of Na⁺ for H⁺ destabilizes folded states, 87
- Post-source decay
- Determination of copper binding sites in peptides containing basic residues: a combined experimental and theoretical study, 31
- Predissociation
- Photodissociation measurements of bond dissociation energies: *D*₀(Al₂-Al), *D*₀(TiO⁺-Mn), and *D*₀(V₂⁺-V), 143
- Proteins
- Gas-phase ion/ion interactions between peptides/proteins and iron ions in a quadrupole ion trap, 47
- Proteolysis
- Probing protein–metal ion interactions by electrospray ionization mass spectrometry: enolase and nucleocapsid protein, 113
- Quadrupole ion trap
- Determination of alkali metal binding selectivities of caged crown ligands by electrospray ionization quadrupole ion trap mass spectrometry, 133
 - Dissociation mechanisms for metal N-glycosides of N-acetyl neuraminic acid, 185
- Radiative association
- Reactions of multidentate ligands with ligated alkali cation complexes: self-exchange and “sandwich” complex formation kinetics of gas phase crown ether–alkali cation complexes, 171
- Rare gases
- Determination of weak Fe⁺–L bond energies (L = Ar, Kr, Xe, N₂, and CO₂) by ligand exchange reactions and collision-induced dissociation, 7
- Reaction stoichiometry
- Stoichiometry in zinc ion transfer from metallothionein to zinc finger peptides, 1
- Sequential clustering
- Sigma bond activation by transition metal ions: the Co(CH₄)_n⁺ systems revisited, 281
- SIFT technique
- Coordination chemistry of (*c*-C₅H₅)Fe⁺ in the gas phase at 294 ± K: reactions with the inorganic ligands H₂, H₂O, NH₃, CO, N₂, NO, CO₂, N₂O, and NO₂, 209
- Sodium
- Large anhydrous polyalanine ions: substitution of Na⁺ for H⁺ destabilizes folded states, 87
- Sodium bonding energies
- Associative ionization of excited sodium species with various ligands: assessing relative bonding strengths of ion–ligand interactions, 247
- Solvated Li atom
- Complexes of Li atoms with water and ammonia: a combined neutralization–reionization mass spectrometry and theoretical study, 125
- Stability
- Large anhydrous polyalanine ions: substitution of Na⁺ for H⁺ destabilizes folded states, 87
- Tandem mass spectrometry
- Chiral resolution of D- and L-amino acids by tandem mass spectrometry of Ni(II)-bound trimeric complexes, 159
- Thermochemistry
- Structure and reactivity of the prototype iron–oxide cluster Fe₂O₂⁺, 233
- Transition metal ions
- Dissociation mechanisms for metal N-glycosides of N-acetyl neuraminic acid, 185
 - Investigating the effect of transition metal ion oxidation state on oligodeoxyribonucleotide binding by matrix-assisted laser desorption/ionization Fourier transform ion cyclotron resonance mass spectrometry, 55
 - Sigma bond activation by transition metal ions: the Co(CH₄)_n⁺ systems revisited, 281
- Zinc finger peptides
- Stoichiometry in zinc ion transfer from metallothionein to zinc finger peptides, 1
- Zinc(II) complexes
- Structures and fragmentations of zinc(II) complexes of amino acids in the gas phase. II. Decompositions of glycine–Zn(II) complexes, 267
- Zirconocenes
- Intrinsic reactivity of metal–hydroxide complexes: O–H bond activation and adduct formation in gas-phase reactions of Cp₂ZrOH⁺, 255